

716

00

FILE COPY  
NO. 6

TECHNICAL MEMORANDUMS  
NATIONAL ADVISORY COMMITTEE FOR AERONAUTICS

---

No. 641

---

LIFT DISTRIBUTION AND LONGITUDINAL STABILITY  
OF AN AIRPLANE

By Carl Topfer

Zeitschrift für Flugtechnik und Motorluftschiffahrt  
Vol. 22, No. 12, June 29, 1931  
Verlag von R. Oldenbourg, München und Berlin

THIS DOCUMENT ON LOAN FROM THE FILES OF

NATIONAL ADVISORY COMMITTEE FOR AERONAUTICS  
LANGLEY MEMORIAL AERONAUTICAL LABORATORY  
LANGLEY FIELD, HAMPTON, VIRGINIA

RETURN TO THE ABOVE ADDRESS.

REQUESTS FOR PUBLICATIONS SHOULD BE ADDRESSED  
AS FOLLOWS:

Washington  
October, 1931

NATIONAL ADVISORY COMMITTEE FOR AERONAUTICS  
1724 F STREET, N.W.,  
WASHINGTON 25, D.C.

# NATIONAL ADVISORY COMMITTEE FOR AERONAUTICS

## TECHNICAL MEMORANDUM NO. 641

### LIFT DISTRIBUTION AND LONGITUDINAL STABILITY OF AN AIRPLANE\*

By Carl Töpfer

In resolving the drag of an airplane wing and of an airplane into the induced drag and the drag due to the viscosity of the air (profile drag and structural drag), it is generally assumed that the lift distribution along the span is elliptical and consequently the induced drag is equal to the ideal drag, i.e., equal to the minimum induced drag

$$W_i = \frac{A^2}{\pi q b^2}$$

at the given aspect ratio. This assumption does not apply, however, to the wing alone nor to the whole airplane for that part of the polars which is most important for the constructor. The drag ratios at large angles of attack below the maximum lift  $C_{a_{max}}$  determine the dimensions of the engines, the take-off weight of the airplane and the size of the wings, etc.\*\* Here any calculation based on the above assumption would prove deceptive.

Not only the drag is inaccurately given by the hitherto customary method of calculating the airplane polar, but even the lift in terms of the angle of attack, in particular the maximum lift and hence the minimum horizontal speed. The  $C_{a_{max}}$  determined by a wind-tunnel test with a model enables no sure conclusion regarding the maximum lift attainable on a full-sized airplane at the given speed. This lift is also affected by the propeller slipstream. Airplane pilots know the great difference between the  $C_{a_{max}}$  at full throttle and at idling speed.

---

\*"Auftriebsverteilung und Längsstabilität," from Zeitschrift für Flugtechnik und Motorluftschiffahrt, June 29, 1931, pp. 366-368.

\*\*"Vorträge aus dem Gebiet der Aerodynamik und verwandter Gebiete" (published by Gilles, Hopf and Kármán), 1929, p. 201 ff.

It was hitherto customary to attribute this lift increase directly to the velocity increase in the field of the propeller slipstream. This cannot affect the lift-drag ratio, however, so far as the wing alone is considered. Since the slipstream is chiefly obstructed by the fuselage, it would be expected that the total drag would increase faster than the lift and that the lift-drag ratio would be reduced by the slipstream. This happens only at small angles of attack. In flat gliding (at a large angle of attack and low sinking speed), the slipstream perceptibly improves the lift-drag ratio, namely for airplanes with more than one engine (sudden "pancaking" when the gas is shut off). Moreover, since the great difference in lift between full throttle and idling speed cannot be explained by the velocity increase in the slipstream, I take exception to the hitherto customary explanation that the slipstream affects the lift indirectly in connection with the disturbance of the lift distribution.\*

In an ideal nonviscous fluid the lift distribution is nearly elliptical throughout the span, even on rectangular and tapering wings. In a viscous fluid, however, this lift distribution is maintained only up to a critical angle of attack, when the flow begins to separate at the middle of the wing. The lift distribution is then changed, as shown in Figure 2. In this lift distribution the induced drag is greater than the minimum drag calculated by the formula. This determines the resolution of the measured total into  $C_{wp}$  and  $C_{wi}$ , which explains the exceedingly rapid increase in the apparent profile drag at large angles of attack below that of maximum lift  $C_{a_{max}}$ . The increase in the induced drag, as compared with the ideal drag with elliptical lift distribution, is included in the calculated  $C_{wp}$ . With increasing angle of attack, the disturbed region in the middle of the wing increases and the lift ceases to increase linearly with the angle of attack, while the apparent  $C_{wp}$  increases still more rapidly. Finally, the disturbance spreads over so large a portion of the wing

---

\*Since the direction of the slipstream, at large angles of attack, makes an angle with that of the relative wind, which can reach an angle of about  $10^\circ$ , the resulting angle of attack is considerably decreased in the region of the slipstream and the lift increase from the greater wind velocity is found to be wholly or partially neutralized.

that the lift is no longer increased by increasing the angle of attack.

If there is a natural cause of disturbance (fuselage, lateral engines) in the middle of the wing, the separation of the flow begins sooner than it would with the wing alone. How the change in the lift distribution, due to the fuselage, affects the lift and drag, is shown by the Göttingen wind tunnel investigation of a tailless "Weltensegler" airplane model.\* The exceedingly great drag of the fuselage can be explained only by the disturbance in the lift distribution. The  $C_{a_{max}}$  is simultaneously shifted to a smaller angle of attack and thereby reduced. (Fig. 1.) Since the fuselage lies partly above the wing,\*\* the circulation disturbance in the vicinity of the fuselage covers the whole angle-of-attack range, thus increasing the induced drag, as compared with the ideal drag, even at  $C_a = 0$ . Figure 3 shows the lift distribution at  $C_a = 0$ .

The effect of the slipstream is to carry along the local vortex formations between the wing and fuselage and thus shift the separation of the flow to larger angles of attack. The lift increase is therefore due to the fact that the previously disturbed lift distribution is restored by the slipstream (dash line in Figure 2). This simultaneously raises the upper limit of the attainable lift and explains why, at small angles of attack, the slipstream has but little or no effect on the polar (according to the type of airplane). It also explains the great drag increase from the lateral engines, which is especially great at large angles of attack. It is further obvious that the vortex formation between the wing root and fuselage cannot

---

\*L. Prandtl and A. Betz, "Ergebnisse der Aerodynamischen Versuchsanstalt zu Göttingen," Report III, 1927, p. 122.

\*\*The investigation of a high-wing monoplane with lateral engines (Rohrbach landplane), contained in the same report, does not explain the disturbance of the lift distribution with the same clearness, since the horizontal empennage had also greatly assisted, as evidenced by the longitudinal moments. The induced drag depends on the lift distribution over the whole airplane, i.e., the sum of the lifts of the wing and horizontal empennage. The drag ratios at large angles of attack are then correct only when the longitudinal moment of the airplane model is neutralized (equilibrium polar). The  $C_{a_{max}}$  is also considerably affected by the wrongly supporting tail surfaces.

follow the law of similarity with the same accuracy as the aerodynamic forces  $A$  and  $W$  and that the disturbance of the lift distribution by the fuselage will therefore have a different effect on the wind-tunnel than on the full-sized airplane. In the vicinity of the  $C_{a_{max}}$  the wind-tunnel polar cannot be expected to agree with the polar of a full-sized airplane in flight. The same principle applies to the effect of the slipstream.

It is known that the stability calculation for gliding flight fails at large angles of attack. The downwash from the tail surfaces and also the magnitude and location of the resulting aerodynamic force of the wing are affected by the lift distribution. In these three unknowns also lie the obstacles to the satisfactory calculation of the stability in powered flight.

For gliding flight (thrust = 0) it is suggested that the downwash angle, up to about  $(A/W)_{max}$ , be calculated by the formula for elliptical distribution on the wing

$$\Delta = \frac{2}{\pi} \frac{C_a}{100} \frac{F}{b^2} 57.3 \left[ 1 + \frac{1}{4} \left( \frac{b}{2l} \right)^2 \right]^*$$

At  $C_{a_{max}}$ , on the other hand, the calculation of the downwash angle is based on a rectangular lift distribution.

$$\Delta = \frac{1}{2\pi} \frac{C_a}{100} \frac{F}{b^2} 57.3 \left[ 1 + \sqrt{1 + \left( \frac{b}{2l} \right)^2} \right]^*$$

Intermediate values can then be easily interpolated. (Fig. 4a, curves e and f.)

Stability calculations in powered flight (thrust = drag) cannot be based simply on the gliding-flight polar and the wind velocity at the tail, as increased by the slipstream. A considerably greater stability would thus be obtained in powered flight than in gliding flight, while all flight tests lead rather to the opposite conclusion. This is explained by the hypothesis that the slipstream restores the disturbed elliptical lift distribution on the wing. With this distribution the downwash angle, according to the above formulas, is almost twice as large

---

\*Fuchs and Hopf, *Aerodynamik*, 1922, p. 325.

as in gliding flight if, by way of approximation, a rectangular lift distribution is assumed at  $C_{a\max}$ .

The control and stability diagrams in Figure 4 are intended to give a clearer idea of these rather complicated relations. In the control diagram the moment coefficient  $C_m'$  of the wing with respect to the C.G. of the airplane is plotted against the angle of attack. (Curve a in Figure 4a.) Positive  $C_m'$  denotes, as usual, a forward-tipping moment. The moment coefficient  $C_{mL}'$  of the horizontal empennage with respect to the C.G. of the airplane, likewise plotted against the angle of attack of the wing, is considered positive for a given elevator deflection, when the aerodynamic force on the elevator tends to level off the airplane. With this establishment of the sign of  $C_{mL}'$ , contrary to the usual way, the intersection of the two moment curves for the tail surfaces and the wing yields directly the angle of attack of the moment equilibrant. Of course allowance must also be made for the downwash from the tail surfaces. According to whether the lift distribution at large angles of attack is assumed to be elliptical or rectangular, the same elevator deflection yields two different moment curves for the tail. (Of course only elliptical lift distribution comes into the question at small angles of attack.)

Curve f (fig. 4a) shows that the downwash is diminished by the disturbance of the lift distribution. This moment curve is decisive for gliding flight. Its intersection point l with the curve a yields the angle of attack of the moment equilibrant for the given elevator deflection:

$$C_m' - C_{mL}' = 0$$

For powered flight (thrust = drag), we assumed elliptical lift distribution on the wing and calculated the downwash angle accordingly. In the moment curve of the tail surfaces, the wind velocity, as increased by the slipstream, must also be taken into consideration. This is done by rotating the curve c about its point of intersection with the  $\alpha$  axis. (The tail moment becomes zero at the same angle of attack regardless of the wind velocity.) The velocity increment in the slipstream is assumed to be 41% of the flight speed. The aerodynamic force and the tail moment are then exactly doubled.

The wing moment is likewise increased by the slipstream (curve b). For the given elevator deflection, the moment balance is found by the intersection point 2 of the moment curves b and g of the tail and wing for thrust = drag ( $S = W$ ). The moment balance is therefore at a somewhat larger angle of attack in powered flight than in gliding flight ( $S = 0$ ), intersection 1, although the elevator deflection is the same in both cases.

The aerodynamic moment, referred to the C.G. of the airplane and represented by the difference of the moment coefficients

$$\Delta C_m = (C_m' - C_{mL}')$$

is derived from the control diagram and transferred to the stability diagram. The angle at which the resulting moment curve intersects the  $\alpha$  axis is a criterion for the stability with moment balance

$$\frac{d \Delta C_m}{d \alpha}$$

It is obvious that the stability in powered flight may be less than in gliding flight (the basis of comparison being the same elevator deflection), although the slipstream doubles the aerodynamic force on the tail surfaces.

In conclusion, attention is called to the fact that the conversion of the wing polar measured in the wind tunnel to another aspect ratio is likewise based on the assumption of an elliptical lift distribution. In so far as this assumption does not hold good at large angles of attack, the function  $C_a = f(\alpha)$  in the vicinity of  $C_{a_{max}}$  is not correctly given by the customary conversion formulas.

Summary.— The preliminary calculation of the airplane polar and hence of the flight performances and characteristics rests on the assumption of an elliptical lift distribution at all attitudes. For large angles of attack below  $C_{a_{max}}$ , this method of calculation yields no satisfactory agreement with measurements made in flight. An attempt is made to eliminate the errors in the preliminary calculation by the assumption of a disturbance of the lift distribution in this angle-of-attack range, which is so important for

the constructor. An explanation is also given of the great differences found in flight with and without propeller slipstream.

Translation by Dwight M. Miner,  
National Advisory Committee  
for Aeronautics.

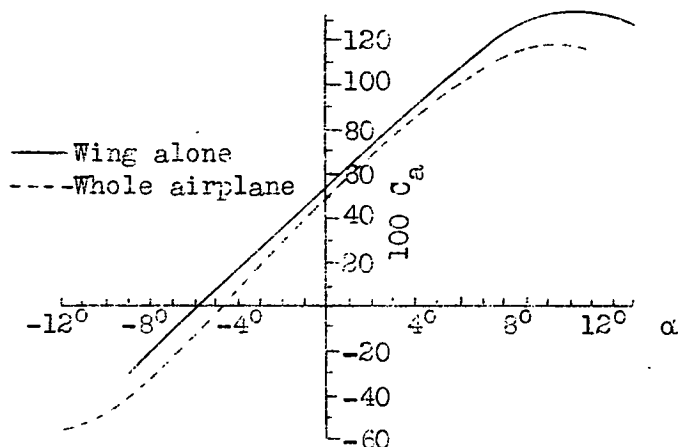


Fig.1 Shifting of function  $C_L = f(\alpha)$  due to disturbance of lift distribution on model of Weltensegler airplane and corresponding wing alone, as shown by Göttingen tests.

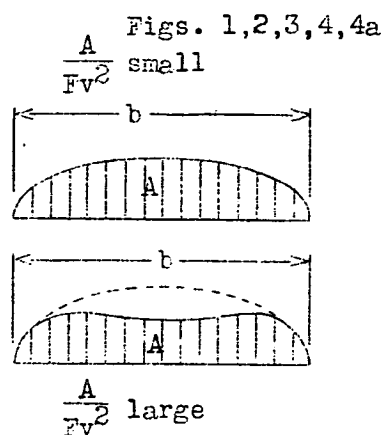


Fig.2 Lift distribution at small and large angle of attack below  $C_{L_{max}}$ .

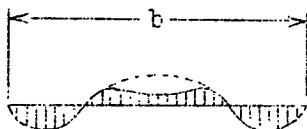


Fig.3 Lift distribution on model of Weltensegler airplane at  $\alpha = -4.5^\circ$ .

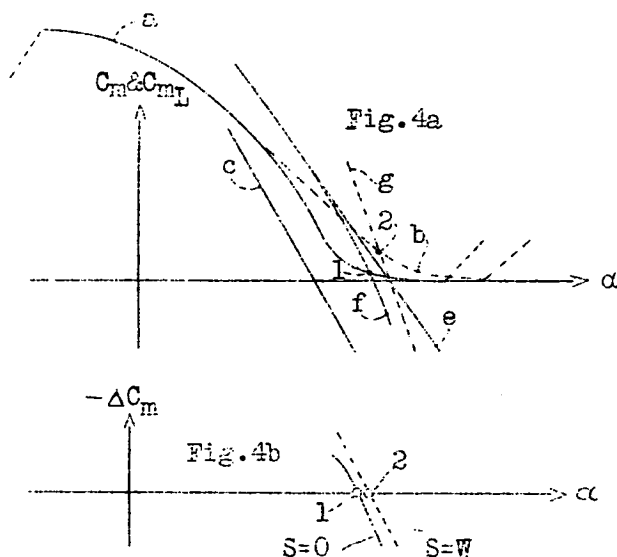


Fig.4 Control and stability diagram for horizontal empennage.